Nickel insertion was performed according to described procedures from nickel(II) acetate by boiling the porphyrin with the nickel source for 30 min in a mixture of glacial acetic acid and methylene chloride, followed by chromatography on silica gel (methylene chloride as eluant) and crystallization from methylene chloride–hexane.[22d-f]

Ni(a-BHP) and Ni(e-BHP) were prepared by reacting the corresponding free-base porphyrin (150 mg) and nickel chloride (300 mg) in refluxing dimethylformamide (10 mL) for 1 h. The organic solution was then evaporated to dryness. The remaining solid was washed with water (×3) and dried (Na_2SO_4). Chromatography on a silica gel column with methylene chloride–acetone (20:1 v/v) gave the expected compounds (120 mg), which were crystallized from methylene chloride–hexane.

Preparation of $^{61}Ni(AcOH)_2$. ^{61}Ni was purchased from CEA (France). HNO_3 was added with stirring to metallic Ni. The resulting green solution of nickel nitrate was then evaporated to dryness. Addition of 0.1 M NaOH to the green residue gave a gelatinous precipitate of $Ni(OH)_2$, which was filtered off. Subsequent treatment of the solid with acetic acid afforded the desired product.

Instrumentation and Procedures. The instrumentation for cyclic voltammetry and thin-layer UV–vis spectroelectrochemistry was the same as previously described.[23] A similar thin-layer cell was used for room-temperature ESR experiments. In both cases the working electrode was a platinum grid. For low-temperature ESR experiments the nickel("I") porphyrin was prepared by electrolysis of 5 cm^3 of a 1–2 mM nickel(II) porphyrin solution in a 35 mm diameter–15 mm high carbon crucible serving as the working electrode. The electrolyzed solution was then transferred under argon pressure to a degazed ESR quartz tube, which was then cooled down to the desired temperature. The ESR spectra were obtained on a ER200E BandX ER 041 MR Brucker spectrometer. The magnetic field was measured with a ER 035 M NMR gaussmeter.

Acknowledgment. J. Courtieu and H. Lariviere (Laboratoire de Chimie Physique de l'Université de Paris-Sud, Orsay, France) and A. Barrault and M. Vandeviver (Laboratoire de Chimie Moléculaire du CEA, Saclay, France) are gratefully thanked for permission to use their ESR instruments and their helpful advice while we were using them.

Registry No. Ni^{II}OEP, 24803-99-4; Ni^{II}MESOP, 15892-09-8; Ni^{II}DEUTP, 15892-10-1; Ni^{II}TPP, 14172-92-0; Ni^{II}(e-(C12)$_2$-CT-TPP), 117687-99-7; Ni^{II}(a-(C12)$_2$-CT-TPP), 117688-00-3; Ni^{I}OEP, 116025-40-2; Ni^{I}MESOP, 117688-03-6; Ni^{I}DEUTP, 117688-04-7; Ni^{I}TPP, 88669-50-5; Ni^{I}(e-(C12)$_2$-CT-TPP), 117688-01-4; Ni^{I}(a-C12)$_2$-CT-TPP), 117688-02-5.

(22) (a) Treibs, A.; Haberle, N. *Justus Liebigs Ann. Chem.* **1968**, *718*, 183. (b) Backer, E. W.; Ruccia, M.; Biwin, A. H. *Anal. Biochem.* **1962**, *8*, 512. (c) Fischer, H.; Orth, H. In *Die Chemie der Pyrroles*; Akademische Verlags-Gesellschaft: Leipzig, Germany; **1937**; Vol. II, p 424. (d) Momenteau, M.; Mispelter, J.; Loock, B.; Bisagni, E. *J. Chem. Soc., Perkin Trans. 1* **1983**, 189. (e) Momenteau, M.; Mispelter, J.; Loock, B.; Lhoste, J. M. *J. Chem. Soc., Perkin Trans. 1* **1985**, 221. (f) McLees, B. D.; Caughey, W. S. *Biochemistry* **1968**, *7*, 642.

(23) Lexa, D.; Savéant, J. M.; Zickler, J. *J. Am. Chem. Soc.* **1977**, *99*, 2786.

Contribution from the Departments of Chemistry, William Marsh Rice University, P.O. Box 1892, Houston, Texas 77251, Auburn University, Auburn, Alabama 36849, and University of Notre Dame, Notre Dame, Indiana 46556

The Pentacoordinate $[Cu^I((imidH)_2DAP)]^+$ Cation: Its Structural Verification, Ligand Rearrangement, and Deceptive Reaction with Dioxygen

John A. Goodwin,[†] Greg A. Bodager,[†] Lon J. Wilson,*[,†] David M. Stanbury,*[,‡] and W. Robert Scheidt*[,§]

Received May 3, 1988

Crystal structures of two cationic copper(I) complexes of a Schiff-base ligand in two isomeric forms, 2,6-bis[1-((2-imidazol-4-ylethyl)imino)ethyl]pyridine [(imidH)$_2$DAP] and 4-methyl-4-[6-(1-((2-imidazol-4-ylethyl)imino)ethyl)pyrid-2-yl]-4,5,6,7-tetrahydro-1*H*-imidazo[4,5-*c*]pyridine [(imidH)(imidH)′DAP] have been solved. The former species is pentacoordinate about copper, while the latter is tetracoordinate. Crystal data for $[Cu^I((imidH)_2DAP)](BF_4)$, $CuF_4N_7C_{19}BH_{23}$ (A): a = 8.279 (5) Å, b = 24.243 (6) Å, c = 11.417 (3) Å, β = 96.18 (3)°, Z = 4 in the monoclinic space group $P2_1/c$. Crystal data for $[Cu^I((imidH)(imidH)'DAP)](BF_4)$, $CuF_4N_7C_{19}BH_{23}$ (B): a = 12.214 (5) Å, b = 12.638 (8) Å, c = 8.24 (2) Å, α = 104.1 (1)°, β = 93.4 (1)°, γ = 115.2 (1)°, Z = 2 in the triclinic space group $P\bar{1}$. Distortions from an idealized trigonal-bipyramidal geometry for the pentacoordinate species are seen in elongated axial Cu–N average bond distances of 2.41 Å and in shorter in-plane Cu–N average bond distances of 1.91 Å. The tetracoordinate structure may be described as a flattened tetrahedron, having two large N–Cu–N bond angles of 132.8 and 140.4°. The pentacoordinate isomer has previously been proposed to form a dioxygen adduct at room temperature in nonaqueous solution, which, under removal of dioxygen, regenerates $[Cu^I((imidH)_2DAP)]^+$. In this work, this regeneration step has been determined by a Toepler pump experiment to proceed *without* significant release of dioxygen under the conditions of the experiment. Thus, the regeneration of copper(I) from oxygenated $[Cu^I((imidH)_2AP)]^+$ proceeds by a pathway more complex than simple release of O_2 from a dioxygen adduct of $[Cu^I((imidH)_2DAP)]^+$.

Introduction

The coordination chemistry of simple copper(I) compounds is of longstanding interest to us because of the ubiquitous involvement of Cu(I) at cuproprotein active sites.[1] In particular, Cu(I) reactivity toward dioxygen[2-4] and Cu(I) participation in biological Cu(II) ⇄ Cu(I) redox chemistry[5] has stimulated our interest in the $[Cu^I((imidH)_2DAP)]^+$ cation,[6] shown schematically in Figure 1A. About 10 years ago,[7] we first reported observations which indicated that the then-presumed pentacoordinate $[Cu^I((imidH)_2DAP)]^+$ cation reacted reversibly with O_2 in solution under ambient conditions. Since then, additional reports by ourselves[2-4] and others[8,9] have further characterized this "reversible" reaction of $[Cu^I((imidH)_2DAP)]^+$ (and its closely related derivatives) with O_2. Meanwhile, other well-characterized synthetic copper(I)

(1) See, for example: (a) Solomon, E. I. In *Copper Proteins*; Spiro, T. G., Ed.; Wiley: New York, 1981; Chapter 2. (b) Urbach, F. L. In *Copper Proteins*; Sigel, H., Ed.; Metal Ions in Biological Systems, Vol. 13; Marcel Dekker: New York, 1981; Chapter 3. (c) Lerch, K. *Ibid.*, Chapter 5. (d) Lontie, R.; Witters, R. *Ibid.*, Chapter 7. (e) Prêaux, G.; Gielens, C. In *Copper Proteins and Copper Enzymes*; Lontie, R., Ed.; CRC Press: Boca Raton, FL, 1984; Vol. II, Chapter 6. (f) Loehr, T. M.; Sander-Loehr, J. In *Copper Proteins and Copper Enzymes*; Lontie, R., Ed.; CRC Press: Boca Raton, FL, 1984; Vol. I, Chapter 5.

(2) Simmons, M. G.; Merrill, C. L.; Wilson, L. J.; Bottomley, L. A.; Kadish, K. M. *J. Chem. Soc., Dalton Trans.* **1980**, 1827.

(3) Merrill, C. L.; Wilson, L. J.; Thamann, T. J.; Loehr, T. M.; Ferris, N. S.; Woodruff, W. H. *J. Chem. Soc., Dalton Trans.* **1984**, 2207.

(4) Goodwin, J. A.; Stanbury, D. M.; Wilson, L. J.; Scott, R. A. In *Biological and Inorganic Copper Chemistry*; Karlin, K. D., Zubieta, J., Eds.; Adenine: Guilderland, NY, 1986, Vol. II, p 11.

[†] William Marsh Rice University.
[‡] Auburn University.
[§] University of Notre Dame.

0020-1669/89/1328-0035$01.50/0

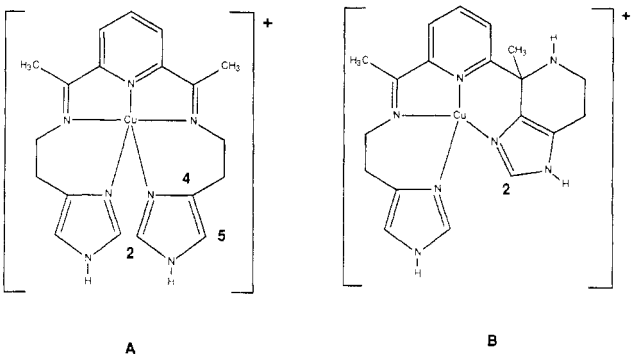

A B

Figure 1. Schematic representations of the copper(I) complexes: (A) $[Cu^{I}((imidH)_2DAP)]^+$; (B) $[Cu^{I}((imidH)(imidH')DAP)]^+$.

species have emerged[10-20] that also have been reported to react reversibly with O_2 to some degree in solution, although the reactions are apparently "reversible" only at temperatures significantly below ambient.

In this paper, we confirm that the $[Cu^{I}((imidH)_2DAP)]^+$ cation is, indeed, a monomeric and pentacoordinate Cu(I) species, structurally similar to its Cu(II) analogue and other related Cu(I) and Cu(II) derivatives.[5,21] However, the structural story of $[Cu^{I}((imidH)_2DAP)]^+$ has recently taken on new complexity by our isolation and identification of a tetracoordinate, isomeric form of the cation, shown schematically in Figure 1B and designated as $[Cu^{I}((imidH)(imidH')DAP)]^+$. The structure of the complex shown in Figure 1B is also reported in this work.

Finally, we report a Toepler pump experiment that demonstrates that the reaction of the complex shown in Figure 1A with dioxygen is not reversible since O_2 is not liberated in significant amount when copper(I) is regenerated. Thus, the $[Cu^{I}((imidH)_2DAP)]^+$ cation does not behave as a simple dioxygen carrier.

Experimental Section

Materials. Propylene carbonate (PC) (Aldrich) was twice distilled at 1 Torr and 110 °C; $CaSO_4$ was added to the flask for the first distillation only. A lower boiling fraction was discarded.[22] Acetonitrile-d_3 used in the NMR experiments was purchased from Aldrich (99% isotopic purity) and used as received. After the solvents were degassed with argon sparge, they were stored in a Vacuum Atmospheres N_2-filled drybox. Diethyl ether was purified by standard methods.[23] Dioxygen was routinely dried by passing it through a column of anhydrous $Mg(ClO_4)_2$.

The copper(II) complex of 2,6-bis[1-((2-imidazol-4-ylethyl)imino)-ethyl]pyridine [$(imidH)_2DAP$] was prepared and recrystallized as previously described and elemental analyses (C, H, N, Cu) for the Cu(II)-BF_4^- salt were as satisfactory as reported previously.[2,3] All elemental analyses in this work were obtained commercially by Galbraith Laboratories, Inc. of Knoxville, TN.

Solutions of $[Cu^{I}((imidH)_2DAP)](BF_4)$ were prepared by anaerobic reductive electrolysis of the Cu(II) compound at a Hg-pool electrode in PC with Bu_4NBF_4 as supporting electrolyte (for the Toepler pump experiment) or at a Pt-mesh electrode with $NaBF_4$ as supporting electrolyte in CH_3CN (all other experiments). The reductions were performed at -550 mV vs Ag/AgCl by using a BAS SP-2 potentiostat, a PAR Model 379 coulometer and an Industrial Scientific Ominscribe strip-chart recorder. For the high concentration bulk electrolyses, a Hg pool electrode was more effective at minimizing electrolysis time. This improved preparative method yielded a product with λ_{max} at 510 nm and $\epsilon \approx 2800$ M^{-1} cm^{-1}. In general, preparation of the Cu(I) compound by electrochemical reduction of $[Cu^{II}((imidH)_2DAP)]^{2+}$ is the preferred method because the Cu(II) derivative can first be purified with little trouble, with the use of Sephadex chromatography if necessary (vide infra). Direct preparation of the Cu(I) compound from $[Cu^{I}(CH_3CN)_4]^+$ is less desirable since the $((imid)_2DAP)$ ligand is not easily isolated in its pure (uncyclized) form.

[Bis(salicylaldehyde) ethylenediiminato]cobalt(II), [Co^{II}(salen)]. Crystalline [Co^{II}(salen)] was prepard by the method of Nishikawa and Yamada,[24] using Schlenk line and drybox techniques as a precaution. The crystalline material was verified by using a Rigaku AFC-5 automated X-ray diffractometer equipped with a Micro Vax II computer and TEXAN software;[25] for a selected single crystal, the observed unit cell parameters for the monoclinic cell were: $a = 26.27$, $b = 7.05$, and $c = 14.33$ Å, with $\beta = 97.94°$, which compared well to the reported values of $a = 26.52$, $b = 7.05$, and $c = 14.36$ Å and $\beta = 98.4°$.[26] Anal. Calcd for $CoC_{16}H_{14}N_2O_2$: C, 59.09; H, 4.34; N, 8.61; Co, 18.12. Found: C, 58.69; H, 4.30; N, 8.46; Co, 17.15.

Crystal Growth. $[Cu^{I}((imidH)_2DAP)](BF_4)$. Approximately 75-100 mg of $[Cu^{II}((imidH)_2DAP)](BF_4)_2$ was electrolytically reduced in 200 mL of CH_3CN with $NaBF_4$ as supporting electrolyte. The resulting deep red solution of the Cu(I) product was lyophilized in a Schlenk flask and transferred into a drybox for manipulation. The solid in the flask was

Table I. Summary of Crystal Data and Intensity Collection Parameters for $[Cu^{I}((imidH)_2DAP)](BF_4)$ and $[Cu^{I}((imidH)(imidH')DAP)](BF_4)$

	$[Cu^{I}((imidH)_2DAP)](BF_4)$	$[Cu^{I}((imidH)(imidH')DAP)](BF_4)$
T, K	294	294
formula	$CuN_7C_{19}H_{23}BF_4$	$CuN_7C_{19}H_{23}BF_4$
fw	499.8	499.8
space group	$P2_1/c$	$P\bar{1}$
a, Å	8.279 (5)	12.214 (5)
b, Å	24.243 (6)	12.638 (8)
c, Å	11.417 (3)	8.24 (2)
α, deg		104.1 (1)
β, deg	96.18 (3)	93.4 (1)
γ, deg		115.2 (1)
V, Å^3	2278.2	1096.8
Z	4	2
d(calcd), g/cm^3	1.46	1.51
radiation	Cu Kα ($\bar{\lambda}$ = 1.5418 Å)	Mo Kα ($\bar{\lambda}$ = 0.71073 Å)
	graphite monochromated	
diffractometer	Enraf-Nonius CAD4[a]	
scan technique	θ-2θ	θ-2θ
no. of unique obsd data	881	1647
R_1	0.131	0.084
R_2	0.147	0.098

[a] Laboratory of W. R. Scheidt, University of Notre Dame.

(5) (a) Goodwin, J. A.; Stanbury, D. M.; Wilson, L. J.; Eigenbrot, C. W.; Scheidt, W. R., *J. Am. Chem. Soc.* **1987**, *109*, 2979. (b) Goodwin, J. A.; Wilson, L. J.; Stanbury, D. M.; Scott, R. A. *Inorg. Chem.*, following paper in this issue.

(6) This abbreviation nomenclature does not follow IUPAC conventions in that diacetylpyridine (DAP) and histamine (abreviated here as imidH) have undergone a Schiff-base condensation to form a new pentadentate ligand, $((imidH)_2DAP)$. This abbreviation scheme has been previously adopted by us[5a] to facilitate abbreviation of future derivatives of $[Cu((imidH)_2DAP)]^{n+}$ that are now under development. The compounds $[Cu((imidH)_2DAP)]^{2+/+}$ have previously had the designations [Cu(imep)]$^{2+/+}$ in the older literature.[2]

(7) Simmons, M. G.; Wilson, L. J. *J. Chem. Soc., Chem. Commun.* **1978**, 634.

(8) Casella, L.; Gullotti, M. *J. Am. Chem. Soc.* **1981**, *103*, 6338.

(9) Casella, L.; Silver, M. E.; Ibers, J. A. *Inorg. Chem.* **1984**, *23*, 1409.

(10) Karlin, K. D.; Cruse, R. W.; Gultneh, Y.; Hayes, J. C.; Zubieta, J. *J. Am. Chem. Soc.* **1984**, 3372.

(11) Karlin, K. D.; Cruse, R. W.; Gultneh, Y.; Hayes, J. C.; McKown, J. W.; Zubieta, J. In *Biological and Inorganic Copper Chemistry*; Karlin, K. D., Zubieta, J., Eds.; Adenine: Guilderland, NY, 1986; Vol. II, p 101.

(12) Karlin, K. D.; Cruse, R. W.; Gultneh, Y.; Farooq, A.; Hayes, J. C.; Zubieta, J. *J. Am. Chem. Soc.* **1987**, *109*, 2668.

(13) Karlin, K. D.; Haka, M. S.; Cruse, R. W.; Gultneh, Y. *J. Am. Chem. Soc.* **1985**, *107*, 5828.

(14) Pate, J.; Solomon, E. I.; Cruse, R. W.; Karlin, K. D. *J. Am. Chem. Soc.* **1987**, *109*, 2624.

(15) Thompson, J. S.; Harlow, R. L.; Whitney, J. F. *J. Am. Chem. Soc.* **1983**, *105*, 3522.

(16) Thompson, J. S.; Whitney, J. F. *Inorg. Chem.* **1984**, *23*, 2813.

(17) Thompson, J. S.; Swiatek, R. M. *Inorg. Chem.* **1985**, *24*, 110.

(18) Thompson, J. S. *J. Am. Chem. Soc.* **1984**, *106*, 8308.

(19) Thompson, J. S. In *Biological and Inorganic Copper Chemistry*; Karlin, K. D., Zubieta, J., Eds.; Adenine: Guilderland, NY, 1986; Vol. II, p 1.

(20) Nishida, Y.; Takahashi, K.; Kuramota, H.; Kida, S. *Inorg. Chim. Acta* **1981**, *54*, L103.

(21) Korp, J. D.; Bernal, I.; Merrill, C. L.; Wilson, L. J. *J. Chem. Soc., Dalton Trans.* **1981**, 1951.

(22) Perrin, D. D.; Armarego, W. L.; Perrin, D. R. In *Purification of Laboratory Chemicals*, 2nd ed.; Pergamon: New York, 1980; p 528, 534.

(23) Fujinaga, T.; Izutsu, I. In *Recommended Methods for Purifying Solvents*; Coetzee, J., Ed.; Pergamon: New York, 1982; p 23.

(24) Nishikawa, H.; Yamada, S. *Bull. Chem. Soc. Jpn.* **1964**, *37*, 8.

(25) Available from Molecular Structure Corp., College Station, TX, 77840.

(26) Brückner, S.; Calligaris, M.; Nardin, G.; Randaccio, L., *Acta Crystallogr.* **1969**, *B25*, 1671.

Table II. Fractional Coordinates and Isotropic Temperature Factors for $[Cu^I((imidH)_2DAP)](BF_4)$

atom	x	y	z	B(iso), Å²
Cu	0.4845 (7)	0.11215 (23)	0.2839 (6)	4.9 (2)
N(1)	0.504 (3)	0.1568 (12)	0.4201 (25)	4.1 (6)
N(8)	0.270 (4)	0.0695 (14)	0.3557 (27)	5.3 (7)
N(16)	0.530 (4)	0.0359 (14)	0.272 (3)	7.0 (9)
N(19)	0.761 (3)	0.1009 (13)	0.2102 (25)	4.9 (7)
N(26)	0.440 (3)	0.1563 (13)	0.1432 (27)	4.6 (7)
C(2)	0.626 (4)	0.1769 (14)	0.499 (3)	4.7 (9)
N(3)	0.585 (4)	0.2032 (14)	0.596 (3)	6.4 (8)
C(4)	0.410 (5)	0.1994 (19)	0.578 (4)	7.4 (12)
C(5)	0.368 (4)	0.1746 (11)	0.4806 (27)	2.8 (6)
C(6)	0.195 (4)	0.1633 (16)	0.427 (3)	5.3 (9)
C(7)	0.156 (4)	0.1016 (16)	0.420 (3)	5.7 (9)
C(9)	0.293 (5)	0.0185 (17)	0.373 (4)	5.1 (9)
C(10)	0.220 (5)	−0.0208 (19)	0.453 (4)	7.0 (11)
C(11)	0.439 (7)	−0.0045 (25)	0.303 (5)	9.4 (15)
C(12)	0.454 (7)	−0.0639 (25)	0.298 (5)	10.8 (16)
C(13)	0.590 (8)	−0.0779 (26)	0.233 (6)	12.6 (20)
C(14)	0.692 (7)	−0.0420 (26)	0.194 (5)	10.6 (17)
C(15)	0.647 (6)	0.0092 (21)	0.202 (4)	6.8 (12)
C(17)	0.745 (6)	0.0565 (23)	0.159 (5)	8.7 (14)
C(18)	0.838 (8)	0.039 (3)	0.050 (7)	17.2 (27)
C(20)	0.834 (4)	0.1505 (16)	0.165 (3)	5.3 (9)
C(21)	0.728 (4)	0.2029 (16)	0.179 (3)	4.8 (8)
C(22)	0.554 (5)	0.1926 (17)	0.091 (4)	5.8 (10)
C(23)	0.511 (5)	0.2152 (18)	−0.021 (4)	5.7 (9)
N(24)	0.355 (4)	0.1893 (13)	−0.0393 (28)	5.0 (7)
C(25)	0.323 (4)	0.1593 (16)	0.048 (3)	4.8 (8)
F(1)	0.1091 (25)	0.2020 (10)	−0.2370 (20)	6.4 (6)
F(2)	−0.1570 (25)	0.1990 (10)	−0.2149 (19)	6.4 (6)
F(3)	0.0098 (26)	0.1283 (10)	−0.1351 (20)	7.2 (6)
F(4)	−0.0510 (26)	0.1425 (9)	−0.3330 (21)	7.3 (6)
B	−0.019 (7)	0.1639 (19)	−0.212 (5)	5.7 (10)

[a] The estimated standard deviations of the least significant digits are given in parentheses.

Table III. Fractional Coordinates and Isotropic Thermal Parameters for $[Cu^I((imidH)(imidH)'DAP)](BF_4)$

atom	x	y	z	B(iso), Å²
Cu	0.80423 (16)	0.28856 (18)	0.61250 (23)	3.7
N(1)	0.8733 (10)	0.1772 (10)	0.6546 (13)	4.3 (2)
N(3)	0.9342 (10)	0.0603 (11)	0.7496 (14)	5.0 (3)
N(8)	0.9817 (9)	0.4331 (10)	0.6568 (13)	3.5 (2)
N(16)	0.7851 (9)	0.4340 (9)	0.7759 (12)	3.1 (2)
N(19)	0.4535 (9)	0.3240 (10)	0.7787 (13)	4.3 (2)
N(23)	0.4789 (10)	0.1809 (10)	0.2862 (13)	4.4 (2)
N(25)	0.6378 (9)	0.2276 (9)	0.4793 (12)	3.4 (2)
C(2)	0.8440 (13)	0.0947 (14)	0.7478 (18)	4.9 (3)
C(4)	1.0240 (12)	0.1191 (14)	0.6645 (18)	4.7 (3)
C(5)	0.9803 (12)	0.1898 (13)	0.5997 (16)	3.9 (3)
C(6)	1.0415 (12)	0.2799 (14)	0.4975 (17)	4.5 (3)
C(7)	1.0871 (12)	0.4115 (13)	0.6057 (17)	4.1 (3)
C(9)	1.0023 (11)	0.5306 (12)	0.7731 (16)	3.3 (3)
C(10)	1.1297 (13)	0.6333 (14)	0.8618 (18)	5.2 (3)
C(11)	0.8919 (11)	0.5412 (12)	0.8225 (15)	3.3 (3)
C(12)	0.8984 (12)	0.6550 (13)	0.9070 (17)	4.1 (3)
C(13)	0.7884 (13)	0.6539 (14)	0.9477 (17)	4.7 (3)
C(14)	0.6785 (12)	0.5451 (13)	0.8974 (16)	4.1 (3)
C(15)	0.6804 (11)	0.4349 (12)	0.8082 (16)	3.4 (3)
C(17)	0.5671 (11)	0.3124 (12)	0.7434 (16)	3.6 (3)
C(18)	0.5762 (12)	0.2217 (13)	0.8405 (17)	4.6 (3)
C(20)	0.3980 (13)	0.3594 (14)	0.6481 (18)	5.2 (3)
C(21)	0.3516 (13)	0.2591 (14)	0.4746 (19)	5.4 (4)
C(22)	0.4570 (11)	0.2317 (13)	0.4414 (17)	3.7 (3)
C(24)	0.5894 (12)	0.1747 (13)	0.3126 (17)	4.2 (3)
C(26)	0.5559 (11)	0.2609 (12)	0.5557 (15)	3.2 (3)
F(1)	0.2453 (8)	0.0609 (10)	−0.2420 (12)	7.3
F(2)	0.1010 (9)	−0.0368 (12)	−0.1106 (13)	8.7
F(3)	0.2755 (13)	−0.0492 (13)	−0.0831 (16)	8.8
F(4)	0.2675 (13)	0.1093 (11)	0.0380 (15)	9.9
B	0.2187 (18)	0.0176 (23)	−0.1056 (27)	4.7

[a] The estimated standard deviations of the least significant digits are given in parentheses.

first moistened with CH_3CN (≤0.5 mL) and finally dissolved in freshly distilled CH_2Cl_2 (≈5 mL). This concentrated solution was filtered and apportioned into 1–2-mL aliquots, which were placed into 5-mL vials. Small volumes of CH_2Cl_2, ranging up to half of the total volume, were then added to each vial. The vials were placed on a warm (35–40 °C) surface in the drybox, and cyclohexane (≤0.2 mL) was layered upon each solution. The vials were capped and left in the dark on the warm surface for 4–6 h, after which crystals began to form. The solutions were then layered with a second, larger volume (≈1 mL) of cyclohexane. After 12–24 h, red crystalline blades were obtained which were used for the structure determination.

$[Cu^I((imidH)(imidH)'DAP)](BF_4)$. Crystals of $[Cu^I((imidH)(imidH)'DAP)](BF_4)$ were obtained serendipitously by a procedure similar to that described above for $[Cu^I((imidH)_2DAP)](BF_4)$, with the only apparent difference being a longer electrolysis time (≥2 h). Reduced compounds prepared in this way produce ^1H NMR spectra consistent with a mixture of products, which probably includes the ligand-arm cyclized material. Also, as discussed below, aged solutions of $[Cu^I((imidH)_2DAP)]^+$ yield NMR spectra of the same sort. A bulk preparation of pure $[Cu^I((imidH)(imidH)'DAP)](BF_4)$ has not yet been achieved.

Crystal Structure Determinations. Crystals of $[Cu^I((imidH)_2DAP)](BF_4)$ and $[Cu^I((imidH)(imidH)'DAP)](BF_4)$ were mounted in an inert-atmosphere box in thin-walled glass capillaries; those of $[Cu^I((imidH)_2DAP)](BF_4)$ were mounted with mother liquor also contained in the capillary. An Enraf-Nonius CAD4 diffractometer equipped with a graphite monochromator was used for data collection.

$[Cu^I((imidH)_2DAP)](BF_4)$. Preliminary examination of a thin red crystal of $[Cu^I((imidH)_2DAP)](BF_4)$ revealed a monoclinic unit cell with parameters given in Table I. In choosing crystals for the structure determination, crystal morphology was the primary characteristic used to distinguish individual samples of $[Cu^I((imidH)_2DAP)](BF_4)$ from $[Cu^I((imidH)(imidH)'DAP)](BF_4)$. Some initial measurements were made with Mo Kα radiation; however, the weak diffraction of the crystalline specimens led to the use of Cu Kα radiation to improve the signal-to-noise ratio.

Intensity data collection of $[Cu^I((imidH)_2DAP)](BF_4)$ was hampered by small crystals of relatively poor quality and the severe radiation sensitivity of the crystals. During the course of the data collection, seven different crystals were examined for possible intensity data measurements. Intensity data were eventually measured on three different crystals and a final data set was realized from measurements on two of these crystals. Periodic examination (every 1 h of data collection) of the identical four intensity standards suggested not only that the crystal decay was anisotropic, but that the decay rates differed significantly from crystal to crystal. The first crystal was used to obtain data to $2\theta = 94.89°$ and the second used for data in the range $83.99 < 2\theta\ 105.09°$. Intensities decreased by 16.5% for the first crystal and 20% for the second crystal. The data from a third crystal, which were collected to $2\theta = 94.89°$, showed intensity loss of 53% and were not used in the final analysis. Data for the first two crystals were corrected for the decay by multiplying by the average value of the decrease in intensity for the four standard reflections for both samples. Clearly, such corrections can only be approximations to the proper values but are the best obtainable. A total of 881 data were considered observed. All data were collected by using Cu Kα radiation with $\bar{\lambda} = 1.5418$ Å. The structure was solved by direct methods[27] and refined by full-matrix least-squares methods to a final isotropic model. At convergence, $R_1 = 13.1\%$ and $R_2 = 14.7\%$. Table I summarizes the data collection parameters, while atomic coordinates for $[Cu^I((imidH)_2DAP)]^+$ are listed in Table II.

$[Cu^I((imidH)(imidH)'DAP)](BF_4)$. Preliminary examination of a thin, red crystal of $[Cu^I((imidH)(imidH)'DAP)](BF_4)$ led to the assignment of a two-molecule, triclinic cell with space group $P\bar{1}$. The centrosymmetric choice was confirmed by the intensity statistics and all subsequent developments in the structure analysis. Lattice constants, reported in Table I, came from the automatic centering of 25 reflections ($\bar{\lambda}$ = 0.710 73 Å). Intensity data were measured to 54° with θ–2θ scans and Mo Kα radiation. Two equivalent forms of data were collected and then

(27) Programs used in these crystal structure studies included local modification of Main, Hull, Lessinger, Germain, Declerq, and Woolfson's MULTAN78, Jacobson's ALLS, Zalkin's FORDAP, Busing and Levy's ORFEE and ORFLS and Johnson's ORTEP2. Atomic form factors were from the following: Cromer, D. T.; Waber, J. T. *International Tables of X-ray Crystallography*; Kynoch: Birmingham, England, 1974; Vol. IV, Table 2.2B. Real and imaginary corrections for anomalous dispersion in the form factor of the copper atoms were from the following: Cromer, D. T. *International Tables of X-ray Crystallography*; Kynoch: Birmingham, England, 1974; Vol. IV, Table 2.3.1. Scattering factors for hydrogen were from the following: Stewart, R. F.; Davidson, E. R.; Simpson, W. T. *J. Chem. Phys.* **1965**, *42*, 3175–3187. All calculations were performed on a VAX 11/730 computer.

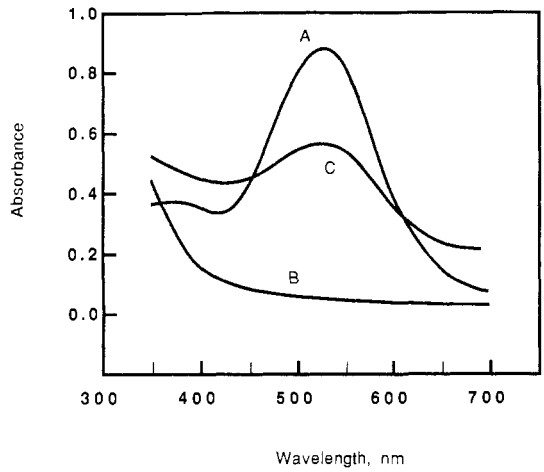

Figure 2. Electronic spectra: (A) the $[Cu^{I}((imidH)_2DAP)]^+$ cation (3 mM, 1 mm path length) in propylene carbonate; (B) the product of the solution used in part A after reaction with O_2 for 3–5 min; (C) the mixture obtained from the solution used in part B, under evacuation, with a recovery time of two hours.

averaged. The averaging R value was 3.1% on F; a total of 1647 averaged data were considered observed and were used in the structure solution and refinement. The structure was solved by direct methods (MULTAN78) and difference Fourier syntheses. Owing to the limited number of data, only the Cu(I) ion and the atoms of the BF_4^- ion were refined with anisotropic temperature factors. The final model had 159 variables and had $R_1 = 8.4\%$ and $R_2 = 9.8\%$. Final values of the atomic coordinates are given in Table III.

Stoichiometry of Dioxygen Consumption. The dioxygen uptake stoichiometry for $[Cu^{I}((imidH)_2DAP)]^+$ in PC was measured by using the Warburg method,[28] with modifications to avoid contamination by water. The previous Warburg experiments for this system[2] were performed with the samples in DMSO, pyridine, 2,6-lutidine, and DMF media and used water as the manometer fluid. These early experiments also used the copper(I) compound prepared by direct addition of $[Cu^{I}(CH_3CN)_4]^+$ to $(imidH)_2DAP$. In the current experiments, DMF, with methyl orange added for visibility, was used as the manometer fluid and the Cu(I) complex was prepared electrochemically from its Cu(II) analogue.

The temperature of the flasks and solutions was maintained with a constant-temperature bath at 25 °C. The manometer was evacuated and refilled with O_2 several times prior to the experiment, and then O_2-saturated DMF was drawn into the manometer under vacuum. The flask volume was refilled with O_2, and a Cu(I) sample was injected into the flask. The manometer levels were then quickly adjusted (10–20 s) under O_2 atmosphere before closing the stopcock on the flask side and opening the manometer end to the air. A thermobarometer filled with DMF was used to correct the manometer readings for changes in ambient temperature and pressure. Corrections for O_2 solubility in PC and DMF were made by obtaining data on solvent blanks.

Measurement of Evolved Dioxygen. Solutions were prepared in which the $[Cu^{I}((imidH)_2DAP)](BF_4)$ concentration was varied from 3 to 20 mM in three separate trials, while the background electrolyte (Bu_4NBF_4) was held at 1 M. Propylene carbonate was selected as the solvent because of its low vapor pressure and low freezing point. The samples were transferred by syringe into an argon-filled 50-mL round-bottom flask equipped with a 1-mm path length quartz cell attached to a side arm by a Viton O-ring joint and a Teflon needle valve. Electronic spectra were recorded for the Cu(I) solutions at this time by using a Cary 210 or Cary 17 spectrophotometer. After the electronic spectrum of the Cu(I) solution was measured (Figure 2A), the sample was sparged with O_2. The reaction, which was obvious by the change in color from deep red to green (Figure 2B), required only about 1 min. For the 20 mM solution, a minor brown precipitate developed and remained in suspension throughout the experiment. The less concentrated solutions were used to minimize this heterogeneity, but all solutions eventually yielded some precipitate. Immediately after the reaction was judged (by the color change) to be complete, the solution was frozen in liquid N_2. At this point, excess O_2 was removed from the sample in 3–4 freeze–pump–thaw cycles on a vacuum line. The samples were warmed to just above melting point in this process. When degassing was completed, the electronic spectrum of the still green solution was quickly taken under static vacuum. A low temperature was not maintained during the recording of the spectrum, but the solution remained green in color, and a spectrum essentially identical with that in Figure 2B was obtained.

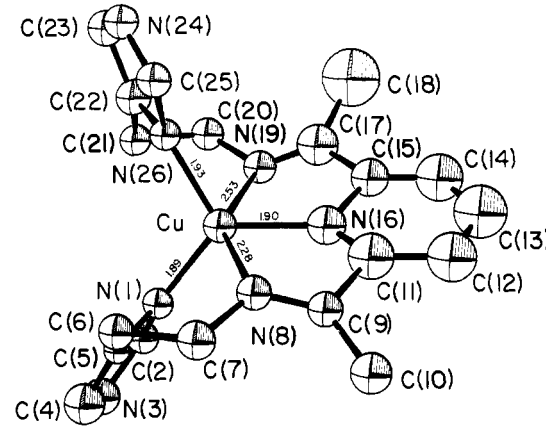

Figure 3. ORTEP drawing of the $[Cu^{I}((imidH)_2DAP)]^+$ cation with the atom-labeling scheme and bond distances in the coordination group displayed. Ellipsoids are contoured at the 30% probability level.

When the sample solution was warmed to room temperature while being subjected to Toepler pumping, the red color returned (Figure 2C). This color change was quite obvious in less than 1 h, but pumping was continued for longer times ranging from 2 to 8 h. The volume of the gas obtained by pumping on the sample was collected, measured, and injected into a Antec 300 gas chromatograph through a direct line from the Toepler pump. A Poropak-Q column ($^3/_{16}$ in. × 28 ft) at −78 °C with helium as the carrier was used to separate the gases. Blanks of air and argon were also passed through the GC since they were considered likely contaminants of the sample gas. The product solutions were filtered in a drybox to remove the light brown solid, and the electronic spectra of the solutions were recorded again.

As a control experiment for the measurement of evolved O_2, the well-known O_2 carrier, $[Co^{II}(salen)]$[26,29–32] was treated under the same conditions as described above for $[Cu^{I}((imidH)_2DAP)]^+$. In noncoordinating solvents such as THF and $CHCl_3$, the dioxygen adduct of $[Co^{II}(salen)]$ does not form at room temperature, and only at −78 °C is the 1:1 adduct completely formed.[32] The compound in PC also shows this type of low-temperature reactivity, so the Toepler pump experiment was carried out under the same conditions given above for the $[Cu^{I}((imidH)_2DAP)]^+$ experiment, except that in the Co(II) case, the oxygenation process was performed at low temperature (−53 °C). Although the extent of formation of the 1:1 ($Co:O_2$) adduct in $CHCl_3$ has been studied at −78 °C, the extent of adduct formation at the slightly higher temperatures of the present work is unknown, and we know of no prior studies of the process in PC. It is probable, however, that under the present condition, adduct formation does not proceed to completion.

A 25-mL solution of $[Co^{II}(salen)]$ at 1.3 mM (3.25 μmol) was prepared in PC. It was exposed to O_2 at 1 atm and −53 °C. The solution turned brown and was allowed to react for 10 min before it was frozen in liquid N_2 for the freeze–pump–thaw cycles prior to the gas evolution measurement. The solution was warmed to room temperature and evolved gas was collected overnight by Toepler pumping. Total yield of gas was 1.28 μmol, which is 39%, assuming complete reaction and a 1:1 stoichiometry. Gas chromatography revealed that 20% of the gas was due to air contamination, which implies a total O_2 yield from the $Co–O_2$ adduct of 32%. This process was then repeated using 25 mL of solution at 0.84 mM (2.1 μmol), with the reaction time extended to 90 min but otherwise treating the sample in a manner identical with the first run. Under these conditions, the yield of O_2 was 7.3 μmol, which implies that the extent of reaction was only 35%.

Analysis of the Final Oxygenation Products. Reaction of $[Cu^{I}((imidH)_2DAP)]^+$ with O_2 in CH_3CN was allowed to proceed for 12 h at room temperature, protected from atmospheric water with a rubber septum. The solvent was removed under vacuum and the brown product extracted with acetone by using ultrasonic agitation. The resulting suspension (≈2 mL) was filtered to separate a dark brown solid. The green filtrate was then slowly passed down a Sephadex LH-20 chromatographic column (1.5 × 45 cm) using acetone as the eluent during a total elution time of

(28) Umbreit, W. W.; Burris, R. H.; Stauffer, J. F. In *Manometric Techniques*, 4th ed.; Burgess: Minneapolis, MN, 1964.
(29) Nishikawa, H.; Yamada, S. *Bull. Chem. Soc. Jpn.* **1964**, *37*, 8.
(30) Achord, J. M.; Hussey, C. L. *Anal. Chem.* **1980**, *52*, 601.
(31) Calvin, M.; Bailes, R. H.; Wilmarth, W. K. *J. Am. Chem. Soc.* **1946**, *68*, 2254.
(32) Tanzher, G.; Aniconi, G., *Nature (London)* **1973**, *241*, 222.

Table IV. Bond Distances (Å) in $[Cu^{I}((imidH)_2DAP)]^+$

Cu-N(1)	1.887 (29)	C(2)-N(3)	1.35 (4)
Cu-N(8)	2.282 (31)	N(3)-C(4)	1.45 (4)
Cu-N(16)	1.895 (33)	C(4)-C(5)	1.28 (5)
Cu-N(19)	2.534 (29)	C(5)-C(6)	1.52 (4)
Cu-N(26)	1.933 (31)	C(6)-C(7)	1.53 (5)
N(1)-C(2)	1.37 (4)	C(25)-N(24)	1.29 (4)
N(1)-C(5)	1.45 (4)	N(24)-C(23)	1.43 (4)
N(8)-C(7)	1.48 (4)	C(23)-C(22)	1.40 (5)
N(8)-C(9)	1.27 (5)	C(22)-C(21)	1.68 (5)
N(16)-C(11)	1.31 (5)	C(21)-C(20)	1.56 (5)
N(19)-C(17)	1.23 (5)	C(9)-C(11)	1.62 (6)
N(19)-C(20)	1.47 (4)	C(11)-C(12)	1.45 (6)
N(26)-C(25)	1.38 (4)	C(14)-C(15)	1.30 (6)
N(26)-C(22)	1.46 (4)	C(12)-C(13)	1.46 (7)
		C(13)-C(14)	1.33 (7)

Table V. Bond Angles (deg) in $[Cu^{I}((imidH)_2DAP)]^+$

N(1)-Cu-N(8)	88.0 (12)	N(1)-C(2)-N(3)	118.5 (33)
N(1)-Cu-N(16)	128.1 (15)	N(26)-C(25)-N(24)	116.7 (33)
N(1)-Cu-N(19)	109.6 (12)	C(2)-N(3)-C(4)	100.8 (33)
N(1)-Cu-N(26)	111.0 (10)	C(25)-N(24)-C(23)	113.4 (32)
N(8)-Cu-N(16)	75.6 (14)	N(3)-C(4)-C(5)	109.2 (38)
N(8)-Cu-N(19)	146.7 (12)	N(24)-C(23)-C(22)	95.6 (32)
N(8)-Cu-N(26)	117.7 (12)	C(4)-C(5)-N(1)	113.8 (34)
N(16)-Cu-N(19)	71.27 (12)	C(23)-C(22)-N(26)	119.6 (36)
N(16)-Cu-N(26)	120.3 (15)	N(1)-C(5)-C(6)	119.9 (29)
N(19)-Cu-N(26)	83.1 (10)	N(26)-C(22)-C(21)	113.4 (33)
C(2)-N(1)-C(5)	97.7 (29)	C(4)-C(5)-C(6)	126.3 (34)
C(7)-N(8)-C(9)	122.1 (36)	C(23)-C(22)-C(21)	126.9 (35)
C(11)-N(16)-C(15)	104.4 (38)	C(5)-C(6)-C(7)	112.4 (31)
C(17)-N(19)-C(20)	125.3 (42)	C(22)-C(21)-C(20)	105.8 (30)
C(22)-N(26)-C(25)	94.6 (32)	C(6)-C(7)-N(8)	113.4 (32)
Cu-N(1)-C(2)	137.7 (25)	C(21)-C(20)-N(19)	112.2 (28)
Cu-N(1)-C(5)	124.2 (22)	N(8)-C(9)-C(11)	111.5 (41)
Cu-N(8)-C(7)	120.2 (25)	N(19)-C(17)-C(15)	122.6 (53)
Cu-N(8)-C(9)	112.9 (28)	N(8)-C(9)-C(10)	131.1 (41)
Cu-N(16)-C(11)	126.0 (35)	N(19)-C(17)-C(18)	124.9 (56)
Cu-N(16)-C(15)	127.8 (31)	C(10)-C(9)-C(11)	117.2 (40)
Cu-N(19)-C(17)	101.6 (33)	C(18)-C(17)-C(15)	112.1 (53)
Cu-N(19)-C(20)	116.8 (22)	C(9)-C(11)-N(16)	110.9 (46)
Cu-N(26)-C(22)	126.8 (26)	C(17)-C(15)-N(16)	104.6 (44)
Cu-N(26)-C(25)	137.4 (28)	N(16)-C(11)-C(12)	133.1 (53)
C(15)-C(14)-C(13)	113.8 (61)	C(11)-C(12)-C(13)	108.8 (54)
C(12)-C(13)-C(14)	125.4 (65)	N(16)-C(15)-C(14)	131.7 (52)

27 h. This general method has proven to be effective at separating the various analogue compounds of the $[Cu(L_2DAP)]^{2+}$ family.

Results

Crystal Structure Determinations. The overall perspective view of the $[Cu^{I}((imidH)_2DAP)]^+$ cation, shown in Figure 3, illustrates the atom-labeling scheme and Cu-N bond distances. Complete bond distance values are given in Table IV, with the bond angles listed in Table V. As with the previously reported results for the analogous $[Cu^{I}((py)_2DAP)]^+$ complex,[5a] this structure is also clearly pentacoordinate about the Cu(I) ion and may be best described as a trigonal bipyramid with the pyridine nitrogen and imidazole nitrogens defining the trigonal plane. In this case, however, the bond angles of the central plane are significantly distorted from the ideal 120° as seen in Table V: N(1)-Cu-N(16) = 128.1 (15)°, N(1)-Cu-N(26) = 111.1 (10)°, and N(16)-Cu-N(26) = 120.3 (15)°. The angle between the axial imine nitrogens is 146.7 (12)°, similar to that seen in the $[Cu^{I}((py)_2DAP)]^+$ cation (148.5 (6)°) but less than the ideal 180°. The average bond distance to the three trigonal atoms is 1.905 (31) Å, or much less than the 2.070 (33) Å value obtained for the $[Cu^{I}((py)_2DAP)]^+$ cation. However, the 2.408 (30) Å average distance of the Cu-N(imino) bonds is substantially larger than the 2.257 (14) Å average in the analogous $(py)_2DAP$ structure where the difference in bonding interactions between axial and equatorial nitrogens is less exaggerated. These long axial interactions are critical to the assignment of the geometry to a quasi-trigonal-bipyramidal structure since they define the unique axis. As shown in Figure 4, this structure may be compared with that of the Cu(II) derivative obtained earlier,[21] which also shows a pentacoordinate structure, however, more in keeping with a square-pyramidal description. The Cu-N bond lengths for the Cu(I) and Cu(II) derivatives are also listed in Table VI for ease of comparison.

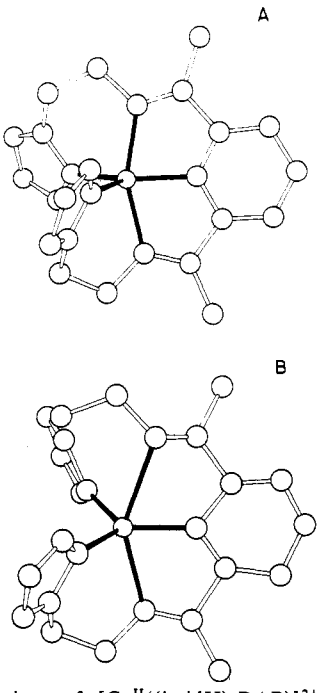

Figure 4. Drawings of $[Cu^{II}((imidH)_2DAP)]^{2+}$ (A) and $[Cu^{I}((imidH)_2DAP)]^+$ (B) illustrating differences in the conformation of the chelated $(imid)_2DAP$ ligand. The DAP plane is in the plane of the page for both molcules. Structure A was drawn from the atomic coordinates reported in ref 21.

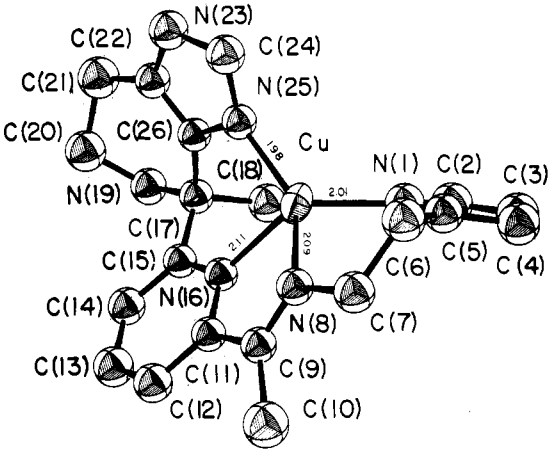

Figure 5. ORTEP drawing of the $[Cu^{I}((imidH)(imidH)'DAP)]^+$ cation with the atom-labeling scheme and bond distances in the coordination group displayed. Ellipsoids are contoured at the 20% probability level.

Table VI. Comparison of Various Cu-N Distances (Å) in the $[Cu^{I,II}((imidH)_2DAP)]^{n+}$ and $[Cu^{I,II}((py)_2DAP)]^{n+}$ Structures

	$[Cu((imidH)_2DAP)]^{n+}$		$[Cu((py)_2DAP)]^{n+}$	
nitrogen atom	Cu^{II} [a]	Cu^{I} [d]	Cu^{II} [b]	Cu^{I} [b]
central pyridine	1.923 (5)	1.90 (3)	1.920 (2)	2.094 (14)
terminal rings	1.992 (5)	1.89 (3)	2.033 (2)	2.032 (12)
	2.081 (6)	1.93 (3)	2.129 (2)	2.083 (12)
imino	2.066 (5)	2.53 (3)	2.026 (2)	2.240 (14)
	2.036 (6)	2.28 (3)	2.010 (2)	2.273 (14)
av[c]	2.020	2.11	2.024	2.144

[a] From ref 21. [b] From ref 5a. [c] Average of five values. [d] This work.

The structure of the $[Cu^{I}((imidH)(imidH)'DAP)]^+$ cation is shown in Figure 5, which also illustrates the atom-labeling scheme and bond distances of the coordination sphere. Complete bond

Table VII. Bond Distances (Å) in $[Cu^{I}((imidH)(imidH)'DAP)]^{+}$

Cu-N(1)	2.006 (11)	C(2)-N(3)	1.346 (15)
Cu-N(8)	2.093 (10)	N(3)-C(4)	1.379 (16)
Cu-N(16)	2.109 (10)	C(4)-C(5)	1.405 (17)
Cu-N(25)	1.981 (10)	C(5)-C(6)	1.544 (18)
N(1)-C(2)	1.382 (16)	C(6)-C(7)	1.517 (18)
N(8)-C(7)	1.489 (14)	C(9)-C(11)	1.481 (15)
N(8)-C(9)	1.279 (14)	C(11)-C(12)	1.403 (16)
N(16)-C(11)	1.367 (14)	C(12)-C(13)	1.399 (16)
N(16)-C(15)	1.326 (13)	C(13)-C(14)	1.397 (17)
N(19)-C(17)	1.494 (14)	C(14)-C(15)	1.418 (16)
N(19)-C(20)	1.490 (16)	C(15)-C(17)	1.512 (16)
N(23)-C(22)	1.381 (15)	C(17)-C(18)	1.585 (17)
N(23)-C(24)	1.394 (14)	C(20)-C(21)	1.543 (20)
N(25)-C(24)	1.343 (15)	C(21)-C(22)	1.492 (17)
N(25)-C(26)	1.371 (13)	C(22)-C(26)	1.341 (16)

Table VIII. Bond Angles (deg) in $[Cu^{I}((imidH)(imidH)'DAP)]^{+}$

N(1)-Cu-N(8)	90.9 (4)	N(1)-C(5)-C(6)	121.5 (11)
N(1)-Cu-N(16)	132.8 (4)	C(5)-C(6)-C(7)	111.1 (11)
N(1)-Cu-N(25)	123.0 (5)	C(6)-C(7)-N(8)	110.3 (11)
N(8)-Cu-N(16)	78.3 (4)	N(8)-C(9)-C(10)	124.9 (11)
N(8)-Cu-N(25)	140.2 (4)	N(8)-C(9)-C(11)	115.8 (11)
N(16)-Cu-N(25)	90.2 (4)	C(10)-C(9)-C(11)	119.2 (12)
C(2)-N(1)-C(5)	108.3 (11)	C(9)-C(11)-N(16)	115.4 (11)
C(2)-N(3)-C(4)	112.1 (12)	C(9)-C(11)-C(12)	121.2 (12)
C(7)-N(8)-C(9)	119.5 (11)	N(16)-C(11)-C(12)	123.3 (11)
C(11)-N(16)-C(15)	119.9 (11)	C(11)-C(12)-C(13)	116.3 (13)
C(17)-N(19)-C(20)	114.6 (10)	C(12)-C(13)-C(14)	120.6 (13)
C(22)-N(23)-C(24)	108.8 (11)	C(13)-C(14)-C(15)	119.1 (12)
C(24)-N(25)-C(26)	107.4 (10)	C(14)-C(15)-N(16)	120.8 (12)
C(2)-N(1)-Cu	133.6 (9)	C(14)-C(15)-C(17)	123.9 (11)
C(5)-N(1)-Cu	117.7 (9)	N(16)-C(15)-C(17)	115.3 (11)
C(7)-N(8)-Cu	121.5 (8)	C(15)-C(17)-C(18)	109.9 (10)
C(9)-N(8)-Cu	115.5 (8)	C(15)-C(17)-N(19)	111.2 (10)
C(11)-N(16)-Cu	112.4 (8)	C(18)-C(17)-N(19)	106.1 (9)
C(15)-N(16)-Cu	126.5 (9)	N(19)-C(20)-C(21)	111.1 (12)
C(24)-N(25)-Cu	132.9 (8)	C(20)-C(21)-C(22)	105.3 (12)
C(26)-N(25)-Cu	118.5 (8)	C(21)-C(22)-N(23)	127.7 (12)
N(1)-C(2)-N(3)	106.4 (11)	C(21)-C(22)-C(26)	126.7 (13)
N(3)-C(4)-C(5)	103.9 (11)	N(23)-C(22)-C(26)	105.4 (11)
C(4)-C(5)-N(1)	109.1 (12)	N(23)-C(24)-N(25)	107.2 (11)
C(4)-C(5)-C(6)	129.2 (12)	C(22)-C(26)-N(25)	111.1 (11)

distances and bond angle values are listed in Table VII and VIII. The structure is unique among the $[Cu(L_2DAP)]^{n+}$ complexes in that it is tetracoordinate about copper. This structural change is due to cyclization by carbon–carbon bond formation within a ligand arm, to give a structural isomer of $[Cu^{I}((imidH)_2DAP)]^{+}$. This cyclization process is known to occur with free Schiff-base ligand[8,9] and apparently occurs over time in solutions of $[Cu^{I}((imidH)_2DAP)]^{+}$ as well.

The tetracoordinate structure yields bond lengths that cover a much smaller range of values than those in the $[Cu^{I}((imidH)_2DAP)]^{+}$ cation. These values are illustrated in Figure 5. The longest Cu–N bond is that of the central pyridine, at 2.109 (10) Å, in contrast to the other pentacoordinate structures in which this is consistently among the shortest of all the bonds. For the $[Cu^{I}((imidH)_2DAP)]^{+}$ cation, this bond distance has a value of 1.895 (33) Å. The shortest Cu–N bond in the tetradentate structure is that to the imidazole on the cyclized side of the complex. This value is 1.981 (10) Å. Overall, the structure may be described as a flattened tetrahedron, having two large bond angles, N(1)–Cu–N(16) = 132.8 (4)° and N(8)–Cu–N(25) = 140.4 (4)°, both substantially larger than the ideal 109.5°.

The Dioxygenation Reaction. Earlier manometry results suggested that a 2:1 Cu:O_2 stoichiometry holds for the initial reaction of $[Cu^{I}((imidH)_2DAP)]^{+}$ with O_2.[2,7] This result, along with magnetic susceptibility, EPR, and EXAFS studies led to the proposal of the formation of a copper–dioxygen adduct ("Cu_2O_2") with a μ-peroxo-like bridge fostering a superexchange pathway between two formally Cu(II) metal centers.[2-4] The initial O_2-consumption stoichiometry was verified here for the PC medium by repeating the Warburg manometry measurements, which had been previously carried out in other media. For a 2-mL sample of $[Cu^{I}((imidH)_2DAP)]^{+}$ at 5.0 mM (10 μmol), the theoretical O_2 consumption at 1 atm is 122 μL (5 μmol). This volume, within 10%, was taken up in ca. 1 h. with a gradual decrease in consumption rate by about 10-fold to less than 10 μL h^{-1}. This period of time should be contrasted with the reported 2–5 min required to observe the 2:1 Cu:O_2 stoichiometry reported earlier.[2] After oxygenation, the solution was bright green. In an effort to determine the long-term dioxygen consumption, reactions were followed up to 24 h. Under these conditions, the stoichiometry seemed to attain at least a 1:1 ratio. At times >24 h, the Warburg method appears unreliable.

In an attempt at product analysis, a $[Cu^{I}((imidH)_2DAP)]^{+}$ solution containing 53 mg (0.106 mmol) of the BF_4^- salt in acetonitrile was allowed to react with O_2 (1 atm) for 12 h at room temperature. Chromatography of this solution resulted in the isolation of 25.5 mg of solid $[Cu^{II}((imidH)_2DAP)](BF_4)_2$(41% yield). For the present, the brown precipitate that formed remains uncharacterized except for its elemental analysis. Anal. Found: C, 22.36; H, 3.46; N, 11.43; F, 10.08.

Recovery of $[Cu^{I}((imidH)_2DAP)]^{+}$. The reaction between $[Cu^{I}((imidH)_2DAP)](BF_4)$ and O_2 and the subsequent regeneration reaction of Cu(I) has been previously characterized, primarily by spectrophotometry.[2-4] Figure 2 shows the spectra of the Cu(I) species, the product after a few minutes' reaction with O_2, and the resulting solution after sparging with argon or by evacuation of the PC solution. The recovery rate has approximately a second-order dependency upon the concentration of Cu(I) in the original solution. Qualitatively, therefore, a PC solution 5 mM in Cu(I) will take 2–3 h to fully regenerate, whereas a similar solution at 1 mM will take from 24 to 36 h. The apparent limit of recovery, independent of concentration and reversal time, is ca. 67%. Although this value is somewhat less than the 80% reversal reported in the early studies, comparison of the present spectra with those obtained earlier shows that the recovery of $[Cu^{I}((imidH)_2DAP)]^{+}$ is better defined, making the peak at λ_{max} (510 nm) more distinct in the final spectrum for one cycle of the reaction with reversal.

After our early reports of the dioxygen reaction with $[Cu^{I}((imidH)_2DAP)]^{+}$ and related molecules,[2,7] Casella et al. reported[9] reactivity of dioxygen with a similar Cu^{I} complex having methyl ester linkages at the C(7) and C(20) carbons of the current study (Figure 3). Their studies confirmed a 2:1 (Cu:O_2) reaction stoichiometry for the system, and except for minor differences, the spectroscopic results for the methyl ester derivative reaction with O_2 paralleled those of the $[Cu^{I}((imidH)_2DAP)]^{+}$ cation.

Dioxygen Evolution Measurements. The recovery of $[Cu^{I}((imidH)_2DAP)]^{+}$ was investigated further with regard to the fate of the O_2. This was probed by a Toepler pump experiment because the technique is direct and small quantities of evolved gas can be accurately collected, measured, and identified when coupled with gas chromatography. Three concentrations of Cu(I) (3, 15, and 20 mM) were chosen to test for a concentration effect on O_2 evolution. The highest concentration of 20 mM increased the rate of Cu(I) recovery so the reaction was concluded in less than 1 h. However, the apparently limiting value of ca. 67% recovery, as depicted in Figure 2, was never exceeded, and a brown precipitate was always observed. At the lowest concentration of 3 mM, the reversal reaction took several hours to regenerate the red color. Upon exposure to O_2 (1 atm, 2 min), the $[Cu^{I}((imidH)_2DAP)]^{+}$ solution (20 mM in PC) turned green. Upon cooling, a green precipitate appeared, which could be redissolved with agitation in an ultrasonic bath and warming to room temperature. Under Toepler pumping for 1 h at room temperature, the characteristic red color of the Cu(I) complex reappeared (ca. 67% recovery of the original 510-nm band) with the evolution of 2.3 μmol of gas. This gas was determined to be mostly air by GC detection of N_2, with the observed yield of evolved O_2 being <2% of theoretical, assuming a 2:1 Cu:O_2 stoichiometry. This procedure was repeated by using 7.5 mL of a 15 mM $[Cu^{I}((imidH)_2DAP)]^{+}$ solution. In this case, the yield of gas was 4.8 μmol or 8.5% of theoretical. GC analysis showed the gas to be O_2-enriched air with an estimated yield of evolved O_2 of only 4%. The usual brown

precipitate was observed, and the recovery of Cu(I) as measured by the 510 nm band was 53%. A third measurement was performed with 45 mL of a 3 mM solution. Eight hours were allowed for the collection of gas, and the solution regenerated Cu(I) to ca. 67%. The evolved gas measurement gave 7.2 μmol with a 1:3 N_2:O_2 ratio, implying that the amount of evolved O_2 was 5.4 μmol or 8% of theoretical. GC analysis revealed additional contamination by argon (introduced during initial sparging) but quantitation was hindered because of the similar retention times of O_2 and Ar. However, a rough estimate of 20% Ar contamination led to an estimated yield of O_2 of 6.4%. Because of the slow ligand rearrangement in solution, the $[Cu^{I}((imidH)_2DAP)]^+$ samples for the present Toepler pump experiments were prepared electrochemically in situ as rapidly as possible (Hg-pool electrode) and used immediately in the presence of supporting electrolyte. The possible effect of supporting electrolyte in high concentration (1 M Bu_4NBF_4) on O_2 evolution was checked by obtaining parallel data for the control system, $[Co^{II}(salen)]$ in PC, in the presence and absence of Bu_4NBF_4 with only a small difference in the amount of O_2 evolved (25% with electrolyte vs 32% without electrolyte).[33] In summary, the three Cu(I) experiments have shown that under varying conditions, the average yield of dioxygen was less than 4% and never exceeded 6.4%.

Discussion

Crystal structures of the $[Cu^{II}((imidH)_2DAP)]^{2+}$ and $[Cu^{I/II}((py)_2DAP)]^{n+}$ cations have been previously reported,[5a,21] and the three structures share several features with the present $[Cu^{I}((imidH)_2DAP)]^+$ pentacoordinate complex. In general, the two pentadentate ligands, $(imidH)_2DAP$ and $(py)_2DAP$ (differing only in their terminal imidazole (imidH) or pyridine (py) moieties), envelop the metal ions in the same fashion, regardless of oxidation state. However, the details of the coordination polyhedra of the 1+ and 2+ oxidation states are best described in somewhat different terms. The difference in the average Cu–N bond distances between $[Cu^{I}((py)_2DAP)]^+$ and $[Cu^{II}((py)_2DAP)]^{2+}$ is 0.12 Å, while for the $[Cu^{I/II}((imidH)_2DAP)]^{n+}$ pair, the difference is only 0.086 Å. These Cu–N distance changes occur in a quite asymmetric fashion in both cases, as shown in Table VI. Moreover, a comparison of the dihedral angles between equivalent planes in the complexes presented in Tables IX and X shows that there are genuine differences in the detailed conformations of the two complexes in their two oxidation states. The differences between planes 1–4 in the two redox pairs is particularly notable. Thus, these distortions that are observed in both the $[Cu^{I/II}((py)_2DAP)]^{n+}$ and $[Cu^{I/II}((imidH)_2DAP)]^{n+}$ pairs result primarily from the changes in oxidation state, but with the more pronounced effect seen in the complexes of $(imidH)_2DAP$. Moreover, the pattern in the M–N bond distances in $[Zn^{II}((imidH)_2DAP)]^{2+}$, which characterizes the deviation from an idealized trigonal bipyramid, is again present here in the isoelectronic $[Cu^{I}((imidH)_2DAP)]^+$ case, indicating the importance of ligand control on the final M–N bond distances in these complexes. Finally, and importantly, a comparison between the $[Cu^{I}((py)_2DAP)]^+$ and $[Cu^{I}((imidH)_2DAP)]^+$ structures reveals some differences, but both complexes are monomeric, pentacoordinate Cu(I) species. Thus, the difference in O_2 reactivity toward $[Cu^{I}((imidH)_2DAP)]^+$ and $[Cu^{I}((py)_2DAP)]^+$ (relatively unreactive)[2-4] must arise from rather subtle factors. However, it can be noted that the presence of imidazole moieties in $[Cu^{I}((imidH)_2DAP)]^+$, $[Cu^{I}((imidH)(py)DAP)]^+$, $[Cu^{I}((imidR)_2DAP)]^+$, and $[Cu^{I}((imidR)(py)DAP)]^+$ seems to coincide with the facile O_2 reactivity that is characteristic of $[Cu^{I}((imidH)_2DAP)]^+$.

The ligand rearrangement that yields $[Cu^{I}((imidH)(imidH)'DAP)]^+$ is documented for uncoordinated ligands of this nature,[8,9] but it has not previously been observed in a coordination compound, although we suggested the possibility earlier for these Cu(I) complexes.[4] The role played by the presence of this rearrangement in the reaction of $[Cu^{I}((imidH)_2DAP)]^+$ with dioxygen is not known. In fact, conditions for maximizing the yield of $[Cu^{I}((imidH)(imidH)'DAP)]^+$ with respect to $[Cu^{I}((imidH)_2DAP)]^+$ are also unknown, although ^1H NMR spectra of aged solutions of $[Cu^{I}((imidH)_2DAP)]^+$ develop multiplicity consistent with asymmetric ligand-arm chelation; Figure 6 displays the resulting 90-MHz NMR spectrum after 5 days of aging in CD_3CN under anaerobic conditions. A new Cu(I) complex, $[Cu^{I}((5\text{-}MeimidH)_2DAP)]^+$, presently under study,[33] possesses a methyl group substituent at the 5-position on each imidazole

(33) Coggin, D.; Stanbury, D. M.; Wilson, L. J. Unpublished results.

Table IX. Least-Square Planes for $[Cu^{I}((imidH)_2DAP)]^+$ (A) and $[Cu^{I}((imidH)(imidH)'DAP)]^+$ (B)[a]

	A	B		A	B
	Plane 1: imidH(1)–(N(1)–C(5))				
A	0.0236	−0.3574	C(2)	0.001	0.002
B	0.8694	−0.4211	N(3)	−0.004	−0.013
C	−0.4936	−0.8336	C(4)	0.007	0.018
D	−1.0593	5.8583	C(5)	−0.007	−0.018
N(1)	0.004	0.010	Cu[b]	0.187	0.264
	Plane 2: imidH(2)–(N(26)–C(22))				
A	0.4529	0.5023	C(22)	−0.003	−0.003
B	−0.7888	0.8528	C(23)	0.004	0.014
C	−0.4156	−0.1428	N(24)	−0.003	−0.020
D	2.0918	−1.4446	C(25)	0.001	0.018
N(26)	0.001	−0.009[c]	Cu[b]	−0.273	−0.377
	Plane 3: DAP–C(7)–C(20)				
A	−0.5186		C(13)	0.040	
B	0.0281		C(14)	0.101	
C	−0.8546		C(15)	−0.056	
D	4.6567		N(16)	0.061	
C(7)	−0.263		C(17)	−0.059	
N(8)	−0.329		C(18)	−0.624	
C(9)	−0.036		N(19)	0.446	
C(10)	0.395		C(20)	0.318	
C(11)	−0.031				
C(12)	0.035		Cu[b]	−0.083	
	Plane 4: DAP–(N(8)–N(19))				
A	−0.5477	0.0362	C(13)	0.029	−0.105
B	0.0124	0.5663	C(14)	0.138	0.008
C	−0.8366	−0.8234	C(15)	−0.012	0.118
D	4.7246	4.6866	N(16)	0.070	0.144
N(8)	−0.389	−0.262	C(17)	0.037	*d*
C(9)	−0.115	−0.017	C(18)	−0.486	*d*
C(10)	0.264	0.251	N(19)	0.550	*d*
C(11)	−0.067	0.006			
C(12)	−0.019	−0.145	Cu[b]	−0.058	−0.018
	Plane 5: N(1), N(16), N(26)				
A	0.9841		N(1)	0.0	
B	0.1668		N(16)	0.0	
C	−0.0615		N(26)	0.0	
D	−3.9599		Cu[b]	0.084	

[a] The planes are described by the four coefficients of the expression: $Ax + By + Cz + D = 0$. [b] The position of the metal (Cu) was not included in the calculation of any of the planes. [c] Atoms for this plane are (in order) N(25), C(26), C(22), N(23), and C(24). [d] Not appropriately included.

Table X. Dihedral Angle (deg) Comparisons in $[Cu^{I,II}((py)_2DAP)]^{n+}$ and $[Cu^{I,II}((imidH)_2DAP)]^{n+}$

	interplanar angles			
planes[a]	M = Cu^{I}(py)	M = Cu^{II}(py)	M = Cu^{II}(imidH)	M = Cu^{I}(imidH)
1–2	64.1	68.8	75.8	62.0
1–3	68.5	66.5	54.1	64.3
1–4	67.8	66.2	54.1	65.7
1–5	71.3	67.4	71.4	78.5
2–3	75.5	81.1	77.4	84.4
2–4	75.3	80.9	77.5	84.8
2–5	74.7	63.5	65.8	70.1
3–4	1.4	0.5	0.1	2.2
3–5	69.2	76.8	78.3	63.1
4–5	70.5	77.3	78.2	61.0

[a] See Table IX for designation of planes.

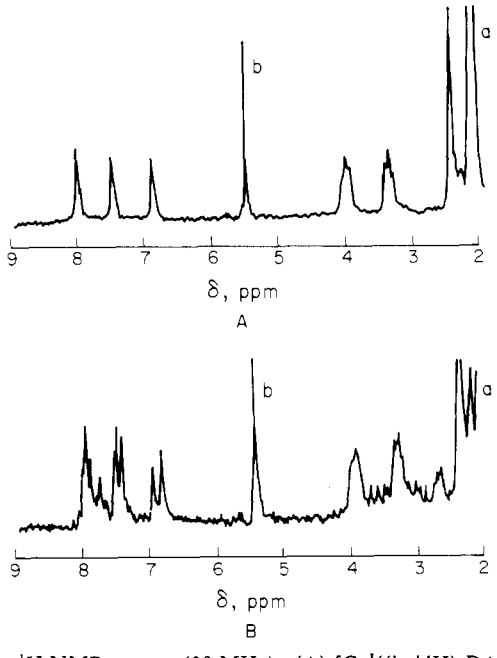

Figure 6. ^{1}H NMR spectra (90 MHz): (A) $[Cu^I((imidH)_2DAP)]^+$ in CD_3CN; (B) sample from part A after it was allowed to stand at room temperature under anaerobic conditions for 5 days. Extraneous peaks are labeled as follows: (a) supporting electrolyte, $(CH_3)_4NBF_4$;[5b] (b) contaminant CH_2Cl_2 from the drybox atmosphere.

ring that precludes ligand-arm cyclization of the nature found in $[Cu^I((imidH)(imidH)'DAP)]^+$.

With the realization that the oxygenation of $[Cu^I((imidH)_2DAP)]^+$ does not proceed reversibly as previously thought, the question remains as to the fate of $[Cu^I((imidH)_2DAP)]^+$ and O_2 upon reaction in their 2:1 stoichiometry. The postulated formation of an O_2 adduct as an intermediate ("Cu_2O_2") is still attractive.[4] However, the pathway by which regeneration of $[Cu^I((imidH)_2DAP)]^+$ (or something spectrophotometrically resembling this complex) occurs more likely results by disproportionation of "Cu_2O_2" to yield not only a Cu(I) complex but also $[Cu^{II}((imidH)_2DAP)]^{2+}$ and other unidentified product or products (brown material). The presence of a disproportionation reaction in the present case is supported by the fact that crystals of $[Cu^{II}((imidH)_2DAP)](BF_4)_2$ have been grown from oxygenated solutions of $[Cu^I((imidH)_2DAP)]^+$ (see Experimental Section) and verified to be the parent Cu(II) compound by X-ray diffraction methods. Shepherd and co-workers[34] have recently reported a detailed kinetic investigation of a binuclear vanadium complex with O_2 which also features a disproportionation mechanism that may have analogies to the present copper system. The brown material(s) obtained from oxygenation of the present $[Cu^I((imidH)_2DAP)]^+$ system has, to date, defied definitive identification, but efforts are continuing in this pursuit.[33]

Our earlier claim of reversibility in the oxygenation of $[Cu^I((imidH)_2DAP)]^+$ was based on a consistent set of data that, however, did not include the crucial test of an O_2-evolution experiment of the nature now described in this work. Conditions permitting, Toepler pump methodology offers one of the most direct and conclusive tests of O_2 reversibility, and it should continue to play a significant role in the development of new small molecule chemistry with Cu(I).

Acknowledgment. L.J.W. thanks the Robert A. Welch Foundation (Grant C-627) and the National Institutes of Health (Grant GM-28451) for support, D.M.S. thanks the NSF (Grant CHE-8520515) and the Robert A. Welch Foundation (Grant C-846) for support, and W.R.S. thanks the NIH (Grant GM-38401) for support. The Rigaku AFC-5 diffractometer at Rice was funded in part by an instrumentation grant from the National Science Foundation.

Registry No. $[Co^{II}(salen)]$, 14167-18-1; $[Cu^I((imidH)_2DAP)](BF_4)$, 75688-52-7; $[Cu^{II}((imidH)_2DAP)](BF_4)_2$, 82135-65-7; $[Cu^I((imidH)(imidH)'DAP)](BF_4)$, 117687-30-6; $(imidH)_2DAP$, 68940-73-8; (imidH)(imidH)'DAP, 117687-28-2; O_2, 7782-44-7.

Supplementary Material Available: Table SI, listing anisotropic temperature factors for $[Cu^I((imidH)(imidH)'DAP)]^+$ (1 page); listings of observed and calculated structure amplitudes for $[Cu^I((imidH)_2DAP)]^+$ and $[Cu^I((imidH)(imidH)'DAP)]^+$ (9 pages). Ordering information is given on any current masthead page.

(34) Myser, T. K.; Shepherd, R. E., *Inorg. Chem.* **1987**, *26*, 1544.

Contribution from the Departments of Chemistry, William Marsh Rice University, P.O. Box 1892, Houston, Texas 77251, Auburn University, Auburn, Alabama 36849, and University of Georgia, Athens, Georgia 30602

Ligand-Substitution and Electron-Transfer Reactions of Pentacoordinate Copper(I) Complexes

John A. Goodwin,[†] Lon J. Wilson,*[,†] David M. Stanbury,*[,‡] and Robert A. Scott[§]

Received May 3, 1988

The kinetics of the electron self-exchange for the Cu(I)/Cu(II) couple of the pentacoordinate complex of 2,6-bis[1-((2-imidazol-4-ylethyl)imino)ethyl]pyridine ($(imidH)_2DAP$) has been studied in CD_3CN by dynamic NMR line-broadening techniques. The rate constant, k'_{22}, is 1.31×10^4 M^{-1} s^{-1} at 25 °C and an ionic strength of 22.3 mM (Me_4NBF_4). Correction for ion pairing gives $k''_{22} = 2.8 \times 10^4$ M^{-1} s^{-1} at μ = 38 mM and 25 °C, which is a factor of 10 greater than that for the $[Cu((py)_2DAP)]^{n+}$ analogue. With the use of these two self-exchange rate constants, the Marcus cross relationship accurately predicts the measured cross-exchange rate constant. Transfer of the ligand from $[Cu^I((py)_2DAP)]^+$ to $[Zn^{II}(CH_3CN)_6]^{2+}$ at μ = 20 mM was investigated at 25 °C in CH_3CN by using the stopped-flow technique. With excess Zn(II), saturation kinetics were observed; this behavior is attributed to rate-limiting dissociation of the copper complex with a rate constant of 310 s^{-1}. These results are considered in evaluating the possibility of an inner-sphere mechanism of electron transfer.

Introduction

As the structural details of the Cu(I)/Cu(II) active sites of copper-containing proteins have become better known by X-ray crystallography,[1,2] understanding of the correlations of these structures with their outer-sphere electron-transfer rates has become a realistic goal. While the relatively high electron-self-exchange rate constants (10^4–10^6 M^{-1} s^{-1})[3-5] have been attributed

[†] William Marsh Rice University.
[‡] Auburn University.
[§] University of Georgia.

(1) (a) Guss, J. M.; Harrowell, P. R.; Murata, M.; Norris, V. A.; Freeman, H. C. *J. Mol. Biol.* **1986**, *192*, 361–387. (b) Guss, J. M.; Freeman, H. C. *J. Mol. Biol.* **1983**, *169*, 521–563.
(2) Norris, G. E.; Anderson, B. F.; Baker, E. N. *J. Am. Chem. Soc.* **1986**, *108*, 2784–2785.

0020-1669/89/1328-0042$01.50/0